

LOX/GCH4 Heat Sink Combustion Chamber: Testing and Preliminary Assessment of Experimental Data

F. Battista¹, D. Cardillo¹, P. Natale¹, M. Panelli¹, M. Fragiaco¹

¹CIRA (Italian Aerospace Research Centre) - Via Maiorise, 81043 Capua (CE), Italy

Keywords : LRE, EXPERIMENTAL TESTS, LOX/LCH4,

ABSTRACT

The work described in this paper has been conducted in the framework of the HYPROB Program, which is carried out by the Italian Aerospace Research Centre (CIRA), under contract by the Italian Ministry of Research. The main objective of the Program is developing design and testing capabilities on liquid rocket engines (LRE), with specific regard to LOX/LCH4 technology.

The system line of the project, named HYPROB BREAD, aims at designing, manufacturing and testing a LRE demonstrator, of three tons thrust, based on a regenerative cooling system using liquid methane as coolant. In order to achieve such goal, some breadboards have been designed to investigate major critical phenomena. Among these breadboards, the SSBB-HS, a heat sink single injector thrust chamber, covers an important role because it has been designed with the aim of investigating the injector behaviour, deepening combustion issues and estimating the heat release to the wall.

This paper deals with the SSBB-HS experimental tests, performed in the AVIO/FAST2 facility by means of two successful campaigns where several firing tests were performed at different chamber pressure conditions for steady state duration ranging from 3 to 11 seconds. The test article, made by a copper and a molybdenum alloys adopted for the cylindrical part and the nozzle one, respectively, was equipped with many embedded thermo-couples and pressure transducers in order to estimate both the chamber pressure and the wall temperature distribution.

The assessment of the results has been performed by means of different tools, in order to verify the working points, and assess the data for a fruitful CFD and design tools tuning.

1. INTRODUCTION

Nowadays the possibility of using the oxygen/methane propellants combination is under active investigation because of the low operational costs, if compared with well-known cryogenic propellants combination like liquid oxygen/hydrogen, and because of methane interesting characteristics, like good overall performance from a system point of view, high specific impulse and simple extractability from natural gases. The design and optimization of liquid rocket engines using methane still requires detailed studies in order to understand the dominating physical phenomena of propellant injection, combustion and heat transfer;

moreover, very few experimental data and analytical database can be found in literature.

In this context, the HYPROB Program, carried out by the Italian Aerospace Research Centre, has the main objective to enable and improve National System and Technology capabilities on liquid rocket engines with specific regards on methane. The Program is structured in three main development lines, specifically named System, Technology and Experimental. The first one aims at the design and the development of technology LRE demonstrators, including intermediate breadboards; the technology line concerns R&D in the areas of CFD combustion modelling, thermo-mechanical modelling and materials, and advanced optical diagnostics; the experimental line is to acquire testing capabilities for both basic physics and system-oriented (demonstrators) experimentation. The first implementation of the Program (the system line), named HYPROB BREAD, is aimed at designing, manufacturing and testing a LRE demonstrator (DEMO), of three tons thrust, based on a regenerative cooling system using liquid methane as coolant [1].

In the framework of the HYPROB-BREAD program, whose logic can be realized in Figure 1, single injector combustion chambers (Sub Scale Bread Board SSBB) have been designed and manufactured in order to investigate single injector behaviour, heat transfer to the wall and combustion stability. Specifically, both a calorimetric (SSBB-CC) and a heat-sink (SSBB-HS) version have been conceived; they consist in a single coaxial injector (LOX/GCH4) mounted on an injector head that can be used with the two interchangeable combustion chambers.

The present paper briefly presents different aspects of the design and it is mainly focused on testing activities execution (in AVIO/ASI Fast2 facility) and experimental data assessment for the SSBB-HS.

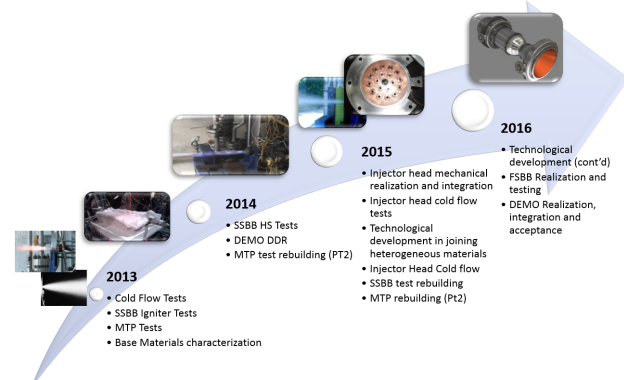


Figure 1: Project time-line [8]

2. DESCRIPTION OF THE SSBB-HS TEST ARTICLE

The SSBB-HS (see Figure 2) consists of three main parts: the injection head, the combustion chamber module made of copper alloy and the throat/nozzle module made of molybdenum alloy in order to withstand the high throat heat fluxes. The combustion chamber is equipped with 12 total embedded thermocouples in 4 different axial stations (visible in Figure 2) and 2 embedded thermocouples in the nozzle throat region, to allow for heat load evaluation. For each station, three thermocouples have been installed at different heights from the chamber wall (an exemplificative image is depicted in Figure 3). Moreover three pressure transducers have been installed for monitoring chamber pressure at different stations (igniter, injection head and end of the cylindrical part of the chamber).

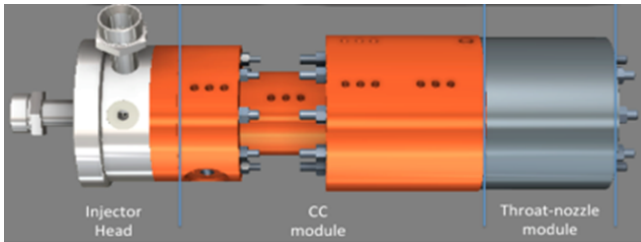


Figure 2: SSBB-HS with visible thermocouples holes

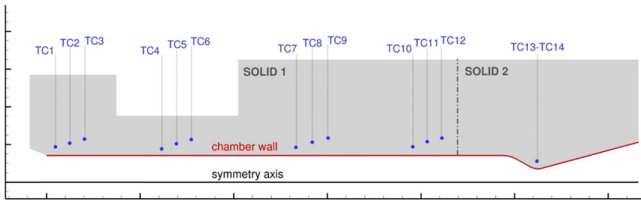


Figure 3: Thermocouples' positioning

As anticipated in the previous section, liquid oxygen and gaseous methane are injected in the combustion chamber by means of a shear coaxial injector with post tip recess, identical to the one that will be installed on the DEMO injection plate.

The objectives of the SSBB-HS are mainly:

- the investigation of the injector behaviour,
- the estimation of the heat flux on the combustion chamber for model validation,
- the implementation of a robust chamber for a first verification of the stability of the combustion [5].

The validation of analytical models by the using of sub-scale testing allows to reduce risks associated with these models in the engine design. Establishing the reliability of design and simulation tools at subscale level, where high fidelity measurements can be performed, is a critical step in gaining acceptance for the use of these tools and realizing the benefits of reduced design cycle times and costs.

IGNITER DESCRIPTION

A customized igniter has been developed and tested for the SSBB combustion chambers [2]. This is a spark torch ignition system that uses two propellants (GOX and GCH₄) that are mixed in the igniter combustion chamber and ignited by a commercial spark plug. The

igniter is made up of two main parts, visible in Figure 4, the igniter head (1) and the torch outlet (2) with flanged interfaces sealed by metal O-rings. The fuel and oxidizer are injected via orifices. The inlet paths of both oxygen and methane are equipped with PT sensors; additionally a pressure sensor is installed in the main chamber in order to monitor chamber pressure [3].

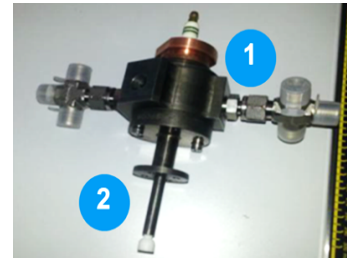


Figure 4: Igniter

Figure 5 shows an exemplificative numerical solution obtained by CFD simulations. Details can be found in [4].

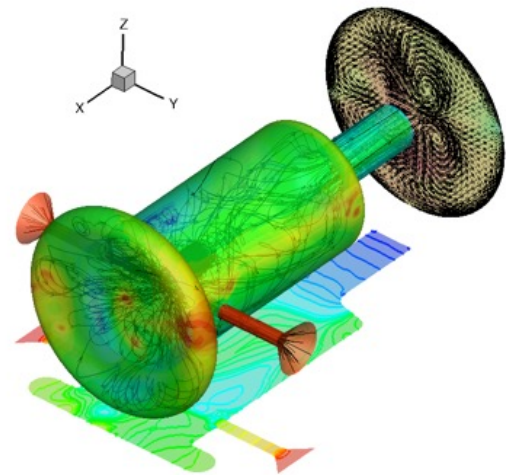


Figure 5: Numerical contour by CFD simulation

The nominal performances of the igniter are reported in Table 1.

Performance	Value
Total Power (kW)	64
Nominal firing time (s)	1.5
Demonstrated shelf life cycles	≥ 20
Chamber pressure (barg)	14

Table 1: Nominal performances of the igniter

3. EXPERIMENTAL TEST CAMPAIGNS

Two experimental test campaigns have been performed in AVIO FAST2 facility. In the first test campaign, after the igniter testing and the ignition testing sequence, 4 tests have been performed:

- 3 at high pressure (nominal Pc about 50 bar) for steady state duration of about 3s;
- 1 at high pressure (nominal Pc about 50 bar) for a steady state duration of 5 s.

In this test campaign 12 thermocouples on the cylindrical part of the chamber have been installed.

In the second test campaign the following tests have been performed (in this test campaign two thermocouples have been added in the throat region):

- 3 at high pressure (nominal Pc about 50 bar) for steady state duration of about 3s (first test campaign repeatability);
- 1 at low pressure (nominal Pc about 28 bar) for a steady state duration of 9 s;
- 2 at low pressure (nominal Pc about 28 bar) for a steady state duration of 11 s.

Test duration has been increased at the end of each test campaign in order to acquire more data in order to rebuild the experimental tests.

It has to be remarked that both methane pressure and oxygen temperature were not perfectly in line with the design values. This caused the injector to work not in nominal condition, but in any case the injector demonstrated wider than expected operative flexibility.

Figure 6 shows the SSBB-HS test article installed on the FAST2 facility test bench, and Figure 7 shows a picture of it during one of the firing tests.



Figure 6: SSBB-HS installed on the test bench in FAST2

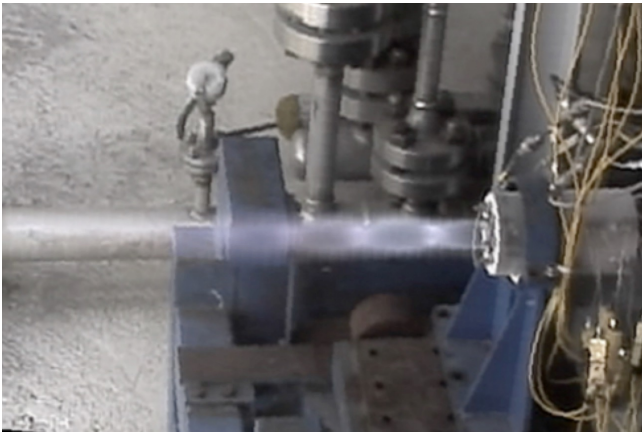


Figure 7: SSBB-HS test article during one of the firing tests

In Figure 8 and Figure 10, temperatures acquired by thermocouples for all the second campaign firing tests are shown [6]. A preliminary mode starts at about 4.5 seconds by using about 10% of the nominal mass-flow rates. After a couple of seconds, full mode conditions are imposed. Due to this switching, a strong increase of curves' slope occurs. Temperatures increase versus firing time until shutdown. Higher values are obtained for thermocouples installed in the nozzle throat (TC13 and TC14). It can be noticed that firing time in full mode conditions is between about 3 and 4 seconds for high-

pressure cases and between about 9 and 11 seconds for low-pressure ones.

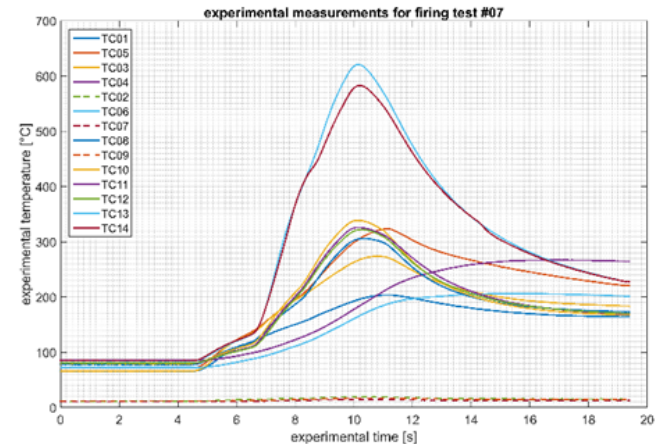
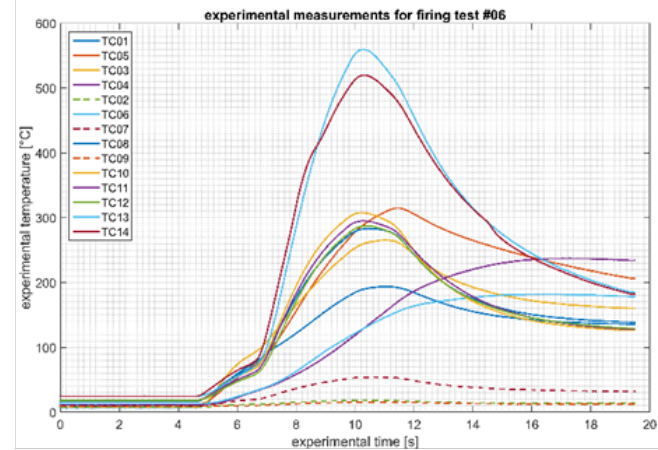
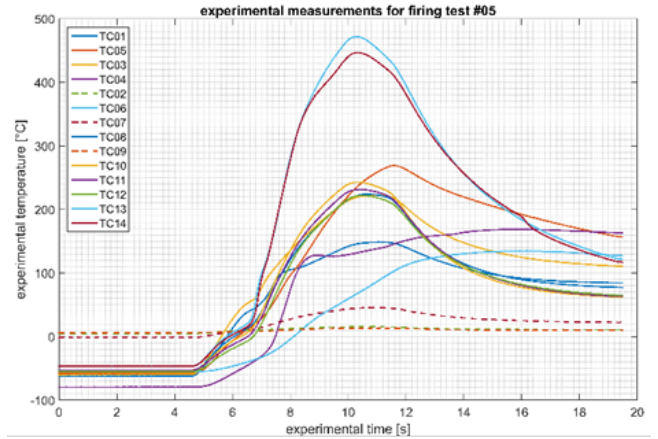


Figure 8: Experimental measurements obtained by thermocouples for all the high-pressure second campaign firing tests

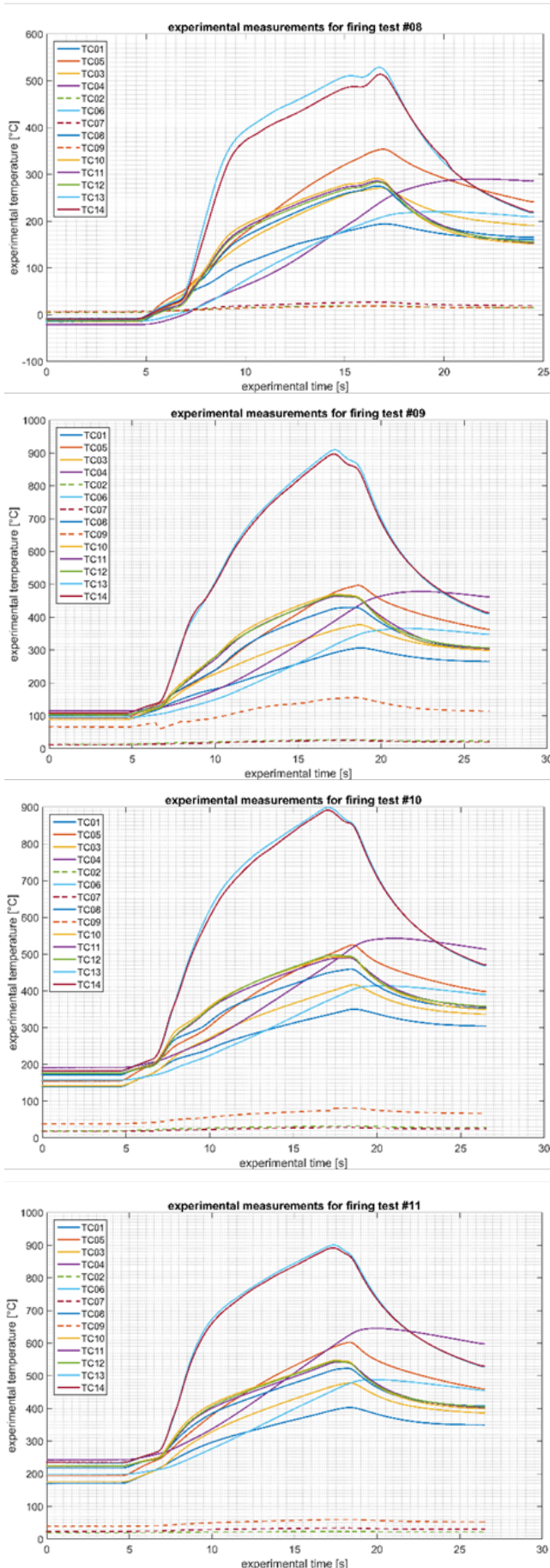


Figure 9: Experimental measurements obtained by thermocouples for all the low-pressure second campaign firing tests

Figure 10 shows measured chamber pressures for all the second campaign firing tests, acquired by one of installed pressure transducers (specifically the one located at the end of the combustion chamber). In full mode operation, chamber pressures are nearly 45 bar for high-pressure firing tests, while these values decrease to about 28-32 bar for the low-pressure cases.

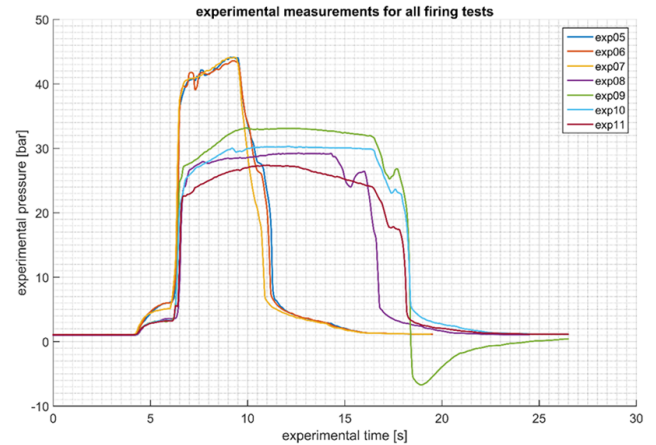


Figure 10: Experimental measurements obtained by pressure transducers for all second campaign firing tests

The test article showed a stable behaviour in all the testing conditions and all the firing tests were successful.

As visible in Figure 8, data by some thermocouples have not been acquired, specifically those represented by the dashed line (TC2, TC7 and TC9). Also data by TC4 and TC6 were unusual, since these thermocouples moved away from their nominal position during the firing test.

Data acquisition of propellants mass flow rates could not be used due to major delay problems related with the facility. These values were therefore obtain a-posteriori by using cold-flow test data, leading to some difficulties in the numerical rebuilding activity and resulting in increased uncertainty margins.

4. EXPERIMENTAL DATA ASSESSMENT

Mixture Ratio

Curves of mixture ratio are reported in Figure 11 for all the firing tests. The time window is limited only in the hot firing-time region. As it can be seen, for high pressure experiments (dashed lines), an actual steady behavior is never reached because of a sort of inertia affecting the feeding lines of the facility. At about 9 sec we can observe a *quasi-steady state* (used for study purposes in this work). For low pressure tests (solid lines), a steady-state behavior is obtained from about 12 sec to 14 sec. This is true except for experiment #10.

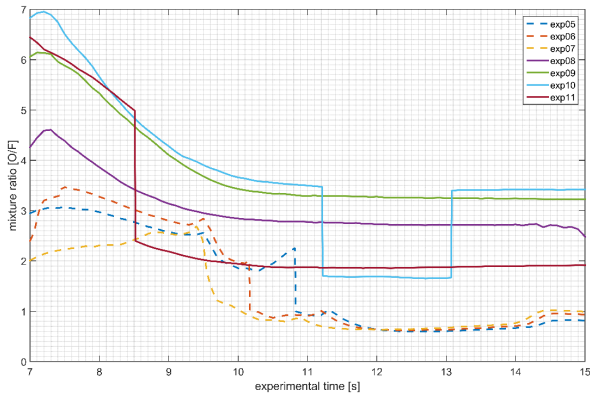


Figure 11: MRs extrapolated for all the experimental tests. Dashed lines represent low pressure experiments; solid lines represent high pressure ones.

In fact, as reported in Figure 12, during the firing-time (into the dashed black circle) the oxygen fluid comes across the transition line. This explains the abrupt transition in phase and then in mass-flow rate, and again in mixture ratio.

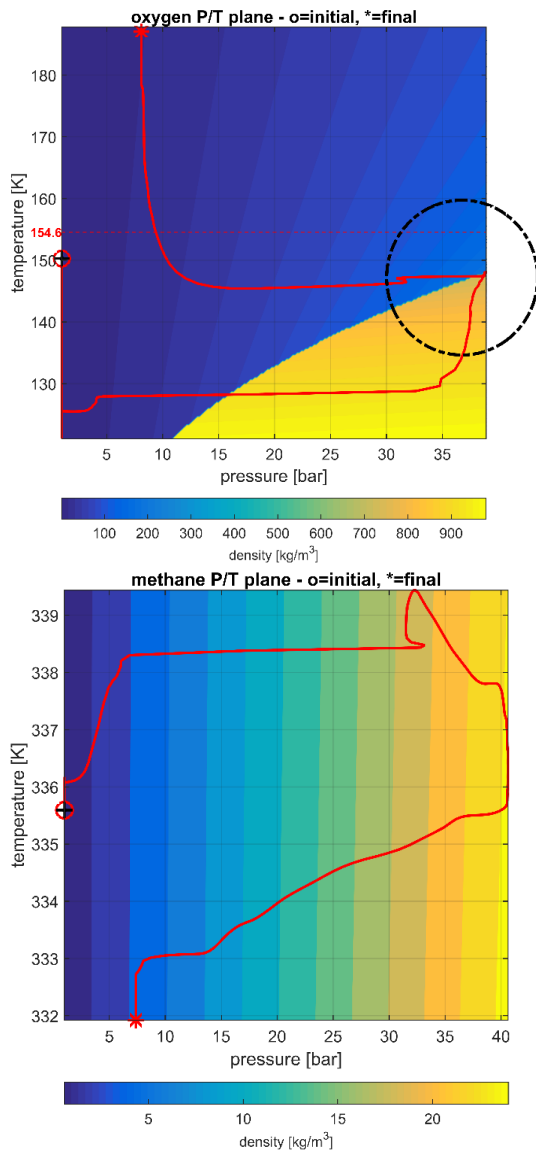


Figure 12: Phase-diagram of propellants with experimental paths (experiment #10)

A prove of this undesired effect comes from experimental combustion chamber pressure measurements. In Figure 13, measurements of combustion chamber pressure are reported, as detected by two different sensors (red-line measurement comes from sensor located in the last part of cylindrical section; blue-line measurement comes from sensor near injection plate). As it can be seen, there is an abrupt decreasing of pressure at about 9.2 sec. This is congruent with a reduction of mixture-ratio (and also of total mass-flow rate) within the injector, as described in Figure 11 and Figure 12. The not-exactly correspondence of the instant of phase transition (11.2 sec in mixture-ratio diagram, vs. 9.2 sec in pressure diagram) may rely on temperature value used for mixture-ratio estimation. In fact, while pressure sensors exhibit only one percent of error in measurement (negligible on phase-diagram), temperature sensors have 5K of tolerance that is significantly important on phase-diagram. For this reason, the extrapolated mixture-ratios and total mass-flow rates, will be furthermore revised.

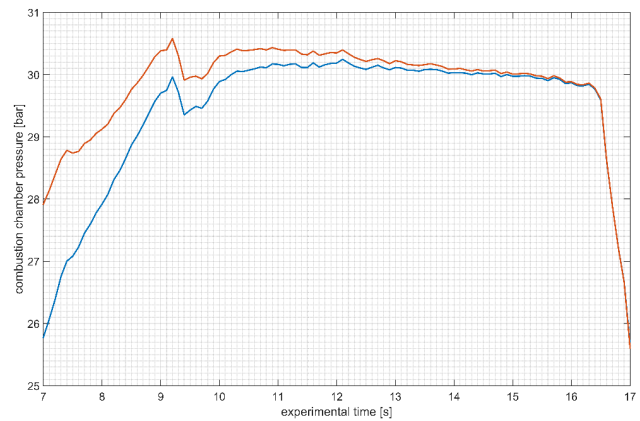


Figure 13: Experimental combustion chamber pressure measurements

Rebuilding of Wall Variables

The methodology developed to calculate temperatures and heat-fluxes on the SSBB-HS chamber wall is described hereinafter, starting from the raw experimental acquisitions. A methodology suggested in literature, specifically by Coy [7], to extrapolate wall heat-fluxes once given temperature measurements by embedded thermocouples was applied. It is based on measurements by two thermocouples (as depicted in Figure 14) at different heights from the chamber wall.

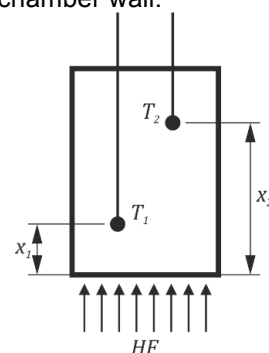


Figure 14: Two measurements are needed by the Coy methodology to re-build wall heat-fluxes

Temperature profiles inside the solid are approximated by using a cubic polynomial expression in x :

$$T_i(x_i) = a + bx_i + cx_i^2 + dx_i^3 \quad \text{Eq. 1}$$

The heat conduction equation is:

$$\frac{\partial T_i}{\partial t} = \alpha_i \frac{\partial^2 T_i}{\partial x_i^2}$$

Where α_i represents the thermal diffusivity.

By replacing T_i in the previous equation, the following expression is derived:

$$\dot{T}_i = \alpha_i(2c + 6dx_i) \quad \text{Eq. 2}$$

Measurements by two thermocouples allow to obtain four equations in the four unknown coefficients:

$$\begin{cases} T_1 = a + bx_1 + cx_1^2 + dx_1^3 \\ \dot{T}_1 = \alpha_1(2c + 6dx_1) \\ T_2 = a + bx_2 + cx_2^2 + dx_2^3 \\ \dot{T}_2 = \alpha_2(2c + 6dx_2) \end{cases}$$

By using the Fourier's law:

$$q = -k \frac{\partial T}{\partial x}$$

The system solving leads to the following expression of the heat flux:

$$q = -k(b + 2cx + 6dx^2) \quad \text{Eq. 3}$$

At the surface, for $x = 0$, heat flux assumes the following expression:

$$q_0 = -k(T_0) \cdot b \quad \text{Eq. 4}$$

A cylindrical coordinates system was introduced, in order to improve the evaluation of temperature profile, taking into account the actual geometry of the solid part.

In cylindrical coordinates, the Laplacian assumes a different form. In particular, considering r in place of x , the following expression has to be used:

$$\nabla^2 T = \frac{1}{r} \frac{\partial}{\partial r} \left(r \frac{\partial T}{\partial r} \right)$$

Where $r = R + x$ (see Figure 15), with R internal wall radius from the axis, x the thermocouple distance from this wall. Using the new expression for Laplacian and assuming the same polynomial expression for temperature profile (as a function of r_i , i.e. radius), the previous equation for temperature rate of change (Eq. 2) becomes:

$$\dot{T}_i(r_i) = \frac{\alpha_i(9dr_i^2 + 4cr_i + b)}{r_i} \quad \text{Eq. 5}$$

It is possible to demonstrate that, starting from Eq. 1, using the definition of r , the Eq. 5 tends to the previous Eq. 2, for $R \rightarrow \infty$. In fact,

$$\begin{aligned} T(x = r - R) &= -R^3d + R^2(c + 3dr) \\ &\quad - R(b + r(2c + 3dr)) \\ &\quad + a + br + cr^2 + dr^3 \end{aligned}$$

$$\begin{aligned} \nabla^2 T(r) &= \dots \\ \dots &= \frac{3 \cdot R^2d - 2R(c + 6dr) + b + 4cr + 9dr^2}{r} \end{aligned}$$

$$\lim_{R \rightarrow \infty} \nabla^2 T(r) = \lim_{R \rightarrow \infty} \nabla^2 T(r = R + x) = \dots$$

Thus, if the chamber radius (i.e. R) is enough greater than x measure, the two expressions are equivalent. In this work, dimension of chamber radii does not allow this assumption. For this reason, the cylindrical expression (Eq. 5) is used in place of the one proposed by Coy (Eq. 2).

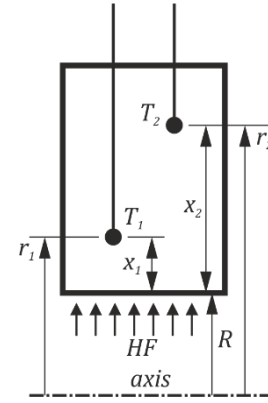


Figure 15: Schematic of variables and positions in cylindrical coordinates

In this case, different values of the four un-knowns are obtained by solving the previous system. In particular, the Eq. 3 becomes:

$$q(r) = -k(b + 2cr + 3dr^2)$$

And Eq. 4 becomes:

$$q_0 = q(r = R) = -k(T_0)(b + 2cR + 3dR^2) \quad \text{Eq. 6}$$

Being more appropriate, Eq. 6 was applied for the test article under analysis.

Some results for firing test #08 are reported in the following figures.

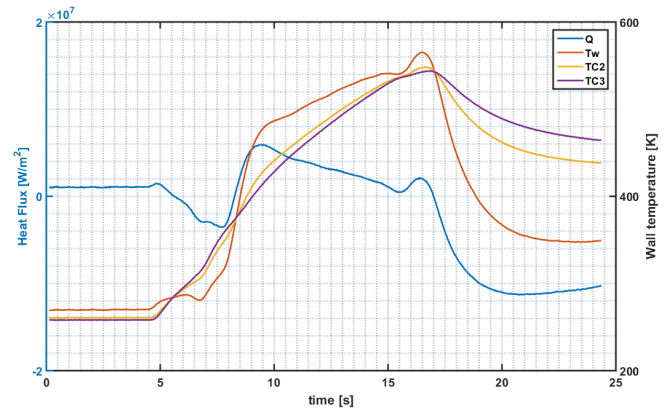


Figure 16: Wall Heat Flux and Temperature in the chamber, in proximity of the firing plate

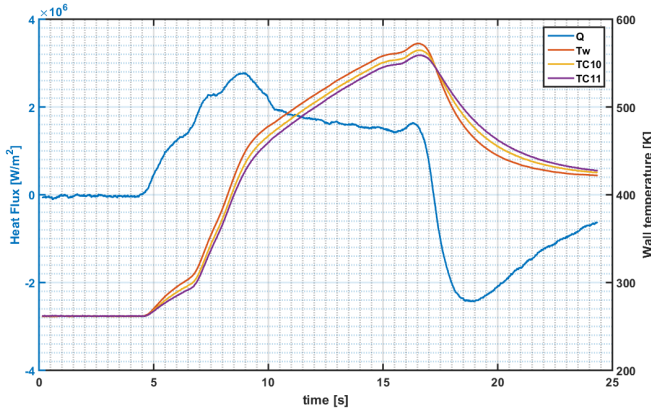


Figure 17: Wall Heat Flux and Temperature in the chamber, before the nozzle

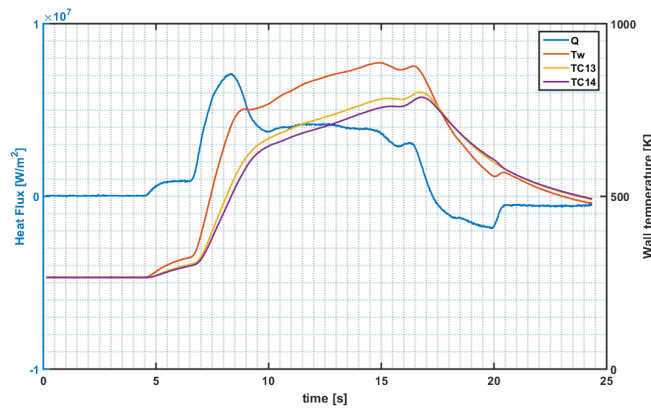


Figure 18: Wall Heat Flux and Temperature in proximity of the nozzle throat

In particular, Figure 16 shows predicted wall heat-flux (blue line) and temperatures (in orange the predicted wall temperature) by considering TC2 and TC3. As it can be seen, a stationary phase cannot be clearly identified. In any case, wall heat-flux increases during the ignition phase and reaches a maximum of about 6 MW/m^2 and then decreases to about 1 MW/m^2 at shutdown. The predicted wall temperature increases to reach its maximum of about 550 K . It is worth to underline that results obtained in this region are affected by some uncertainties due to the limited numbers of sensor installed in this region and a specific study, considering also an improved experiment sensors set-up, should be needed to clarify the behavior in this particular zone of the chamber.

In Figure 17 the second part of the chamber is considered, by means of TC10 and TC11. In this case a stationary wall heat-flux is more visible, with respect to the previous case, when firing time is between 10 and 15 seconds. The predicted wall heat-flux value is about 2 MW/m^2 while the estimated increase to about 550 K at shutdown.

Results of Figure 18 refer to thermocouples in the nozzle throat. It is worth underlying that peak heat-flux is expected in a very narrow region, which could not be in the nozzle throat precise abscissa. In this case the preliminary mode is more visible, leading to slight increase of both wall temperature and heat-flux. Switching to full-mode results in a strong increase of wall heat-flux, which reaches about 7 MW/m^2 . Then a sort of stationary phase can be seen again, with an

average wall heat-flux value of about 4 MW/m^2 . The predicted wall temperature reaches nearly 900 K .



Figure 19: Heat-flux rebuilding for experiment #08

In Figure 19, discarded and selected rebuilt heat-fluxes are reported (exp#08). As abovementioned, only data from thermocouples from TC10 to TC14 were useful for heat-flux reconstruction. Moreover, in order to obtain an evaluation of steady heat-flux, a selected time-window is also reported.

As a consequence, predicted wall heat-flux could not precisely represent the peak values. In Figure 20, experimental rebuilt wall heat-transfer coefficients (red points with uncertainty bars) are compared to a Bartz-like predicted distribution (blue line). Wall temperatures predicted by applying Coy methodology were used in the Bartz-correlation [9] to estimate wall heat-transfer coefficients. As you can see, rebuilt values are strongly underestimated with respect to those predicted by using the correlation. The first two rebuilt values, that are those associated with TC02-TC03 and TC04-TC06, are not considered reliable, thus they should be excluded from comparison.

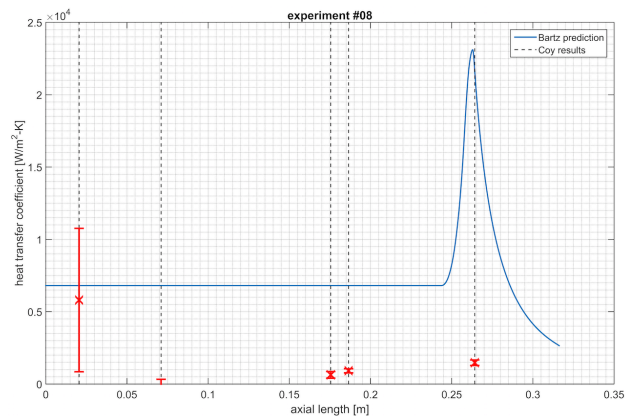


Figure 20: Rebuilt wall heat transfer coefficient Vs. Bartz-like predicted distribution

Remarks on the predicted results

Results obtained by applying the methodology suggested by Coy are considered to be not extremely reliable, specifically underestimated, since the method is based on hypotheses that could introduce significant errors for the SSBB-HS test article under consideration:

1. Temperature profiles are approximated by cubic polynomial expressions
2. Axial component of the heat-flux is neglected with respect to the radial one

For what concern point 1, Figure 21 shows the temperature profiles inside the solid material, obtained by applying the cubic polynomial expression reported in Eq. 1, for the triplet of thermocouples located at the end of the chamber (points represent the experimental data). As you can see, looking at these profiles it's not possible to state that the external wall is adiabatic, on the contrary, a very high heat-flux in this case is predicted. The cubic polynomial expression is an acceptable approximation only in proximity of the thermocouples, considering that the distance between thermocouples and the chamber wall is negligible with respect to the distance between thermocouples and external wall. The SSBB-HS test article does not satisfy the aforementioned hypothesis.

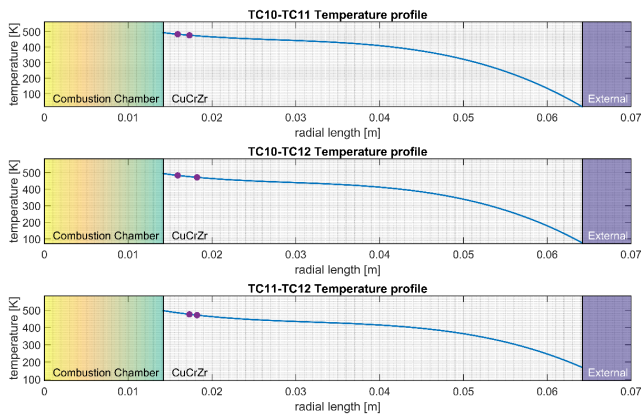


Figure 21: Temperature profiles inside the solid material

Figure 22 shows the CFD temperature prediction in the solid domain with stream-traces by iso-temperature gradient, related to the heat-flux by the Fourier's law, obtained by thermal computation where a heat-flux is applied to the chamber hot-side wall.

As you can see, stream-traces are not normal to the chamber surface, meaning that thermal gradient is different from zero in most part of the domain.

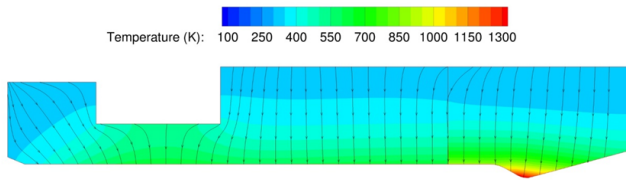


Figure 22: Temperature CFD field with iso-temperature-gradient stream-traces, solution at 7.2 seconds of full mode operation

In Figure 23 the % error associated with the hypothesis of radial heat-flux is computed. As you can see, in the first part of the solid, where the geometry is non uniform, error can reach very high values, of the order of 50% (close to the firing plate). Also in the nozzle throat the hypothesis leads to remarkable underestimation of the heat-flux (of about 10 %), while only in the second part of the chamber the assumption of radial heat-flux is acceptable.

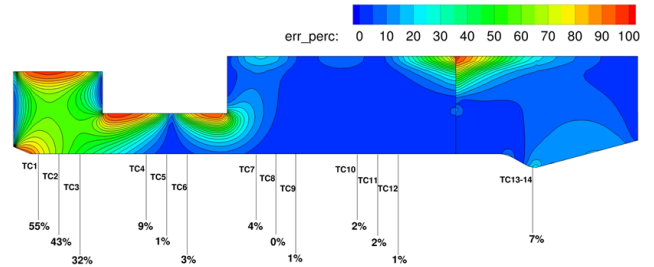


Figure 23: Error in % associated with the hypothesis of radial heat flux (neglecting the axial contribution)

5. FURTHER WORKS

In order to obtain more reliable results a new methodology is being developed in house. This methodology allows an estimation of wall-variables by a single thermocouple measurement, since in some stations only one measurement was available (e.g. measurement by TC8 for the third triplet). In this new methodology temperature profiles inside the solid material are approximated by using a different function. Preliminary results actually show an increase of the predicted wall heat-flux, confirming that the application of the Coy methodology for the case under analysis leads to a slight underestimation of wall fluxes.

6. CONCLUSIONS

In this work all the activities related to the design, manufacturing and testing of the SSBB-HS single injector thrust chamber have been described. Test campaigns were carried out successfully allowing for the collection of data in a wide pressure range. An assessment of experimental data was performed, Propellants mass-flow rates, whose values were not acquired with reliability due to facility problems, were calculated from experimental pressure in order to allow for a numerical rebuilding. Wall variables were rebuilt by means of the Coy methodology, showing some uncertainties related with the applicability of its hypothesis to the test article under analysis. Further works have been initiated in order to obtain more reliable results and a comparison with CFD numerical data.

7. ACKNOWLEDGMENTS

This work has been carried out within the HYPROB program, funded by the Italian Ministry of University and Research (MIUR) whose financial support is much appreciated. Author wants to thank the HYPROB-BREAD project team both CIRA and AVIO side.

8. REFERENCES

- [1] Salvatore, V., Battista, F., De Matteis, P., Rudnykh M., Arione, L., Ceccarelli, F., 2013. *Recent Progress On The Development Of A Lox/Lch4 Rocket Engine Demonstrator In The Framework Of The Italian Hyprob Program*. 64rd International Astronautical Congress, IAC-13,C4,3,4,x19439.
- [2] Sutton, G.P., Biblarz, O., 2010. *Rocket Propulsion Elements*. John Wiley & Sons, ISBN-9780470080245.

- [3] Battista, F., Ferraiuolo, M., Martucci, A., Fragiaco M., Natale, P., Ricci, D., Roncioni, P., French, D.A., Salvatore V., 2014. *Modelling, Testing and Design Considerations of a GOX/GCH₄ Igniter for a HYPROBSSBB Single Injector Thrust Chamber*. Journal of the British Interplanetary Society 01/2014; 67.
- [4] Natale, P., Saccone, G., French, D.A, Battista, F., *Chemical and CFD Modelling of Sub-Scale Bread-Board igniter based on experimental data assessment*, 51st AIAA/ASME/SAE/SEE Joint Propulsion Conference, 27th-29th July 2015, Orlando, Florida.
- [5] Muss J. A., Nguyen T. V., Johnson C. W., 1991, *User's Manual for Rocket Combustor Interactive Design (ROCCID) and Analysis Computer Program*, Volume I, NASA Contractor Report 187109.
- [6] Battista, F., Cardillo, D., Ricci, D., Natale, P., Panelli, M., Fragiaco, M., Salvatore, V., de Matteis, P., *Testing and Preliminary Assessment of Experimental Data of a LOX/GCH₄ Heat Sink Combustion Chamber*, 6th European Conference for Aeronautics and Space Sciences, 29th June – 3rd July 2015, Krakow, Poland.
- [7] Coy, E. B., 2007, *Code validation of CDD Heat transfer models for liquid rocket engine combustion devices*, AFRL-PR-ED-TP-2007-157.
- [8] F. Battista, V. Salvatore, D. Ricci, L. De Rose, *Advancements in the HYPROB-BREAD project: design and testing of a LOX/LCH₄ demonstrator*, Space Propulsion 2016, Roma
- [9] Bartz, D. R. 1957, *A Simple Equation for Rapid Estimation of Rocket Nozzle Convective Heat Transfer Coefficients*, Jet Propulsion 27(1), 49-51.